ORIGINAL PAPER

Electrocatalytic oxidation of hydroxylamine at Ni(II)-morin complex modified carbon nanotube paste electrode

Li Zheng · Jun-feng Song

Abstract A modified electrode, nickel(II)-morin complex modified multi-wall carbon nanotube paste electrode (Ni(II)-MR-MWCNT-PE), has been fabricated by electro-depositing Ni(II)-MR complex on the surface of MWCNT-PE in alkaline solution. The Ni(II)-MR-MWCNT-PE exhibits the characteristic of improved reversibility and enhanced current responses of the Ni(III)/Ni(II) couple compared with Ni(II)-MR complex modified carbon paste electrode (CPE). It also shows better electrocatalytic activity toward the oxidation of hydroxylamine than the Ni(II) modified MWCNT-PE (Ni(II)-MWCNT-PE) and Ni(II)-MR-CPE. Kinetic parameters such as the electron transfer coefficient α, rate constant k_s of the electrode reaction and the catalytic rate constant k_{cat} of the catalytic reaction are determined. Moreover, the catalytic currents present linear dependence on the concentration of hydroxylamine from 2.5×10^{-6} to 4.0×10^{-4} mol L^{-1} by amperometry. The detection limit and sensitivity are 8.0×10^{-7} mol L^{-1} and 56.2 mA L mol^{-1}, respectively. The modified electrode for hydroxylamine determination is of the property of simple preparation, good stability, fast response and high sensitivity.

Keywords Hydroxylamine · Nickel-morin complex · Multi-wall carbon nanotubes · Electrocatalysis

L. Zheng (✉) · J. Song
College of Chemistry and Chemical Engineering, Xi'an Shiyou University, 710065 Xi'an, People's Republic of China
e-mail: lzheng@xsyu.edu.cn

J. Song
Institute of Analytical Science, Northwest University, 710069 Xi'an, People's Republic of China

1 Introduction

Morin (MR, structure shown in Scheme 1) is a flavonoid found in yellow Brazil wood. It possesses biological activities of antioxidant and anti-tumor, almost without side effects and toxicity [1–3]. It can also chelate with some metal cations, such as Cu(II), Co(II), Ni(II) and Cd(II), to form stable complex with scavenging superoxide radical and anti-tumor properties [4, 5]. Therefore, investigating the redox process of MR and the application of environmental friendly material metal-MR complexes are of practical importance. So far, some reports investigate the redox behavior of MR [6], and the interaction of some metal-MR complexes with DNA [7, 8]. However, to the best of our knowledge, there is no report about metal-MR complex modified electrode.

To investigate the application of metal-MR complex modified electrode, hydroxylamine is selected as an object. As known, hydroxylamine is a key intermediate in the nitrogen cycles and production of nitrous oxide [9]. It is also a kind of reducing agents widely used in industry and pharmacy [10]. Moreover, hydroxylamine is a well-known mutagen, toxic and harmful to human, animals, and even plants [11, 12]. Therefore, the quantitative determination of hydroxylamine is important either for industrial, environmental or for biological purposes. Currently, many methods including spectrophotometry [13], chromatography [14, 15], capillary electrophoresis [16] and electrochemical method [17, 18] have been developed for the determination of hydroxylamine. Voltammetric method possesses many advantages as high sensitivity, good selectivity, rapid response and simplicity in operating procedure. It is an alternative for the determination of hydroxylamine. To reduce the large overpotential of hydroxylamine at conventional electrodes [19], various materials such as
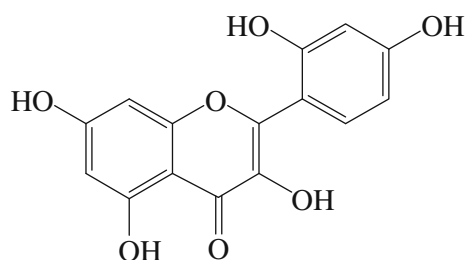
Scheme 1 Structure formula of morin

hexacyanoferrate [20], coumestan [21], rutin [22] and alizarin red S [23] have been used as intermedia for the electro-oxidation of hydroxylamine. Considering that nickel macrocyclic complexes show excellent catalytic activity toward electro-oxidation of some organics containing –OH and –NH$_2$ groups [24, 25], they might also be good catalysts for hydroxylamine oxidation.

On the other hand, carbon nanotubes (CNT) have been widely applied as electrode material due to their high surface area and outstanding ability to mediate fast electron-transfer kinetics for a wide range of electroactive species [26, 27]. CNT composite materials can further enhance electrode's electrocatalytic ability [24, 28, 29]. These composite materials have gained growing interest in the electroanalytical field.

Thus, in the present work, Ni(II)-MR complex and multi-wall carbon nanotubes were both employed to prepare a composite material chemically modified electrode Ni(II)-MR-MWCNT-PE by electrodepositing Ni(II)-MR complex on the surface of multi-wall carbon nanotube paste electrode (MWCNT-PE). The electrochemical behavior of Ni(II)-MR-MWCNT-PE and the electrocatalytic activity to the oxidation of hydroxylamine were investigated by cyclic voltammetry and chronoamperometry.

2 Experimental

2.1 Materials

MR (purity > 98%) was purchased from Shanghai Reagent Factory (Shanghai, China). 1.0×10^{-3} mol L^{-1} MR was prepared in 0.10 mol L^{-1} NaOH solution. The stock solution of 1.0×10^{-2} mol L^{-1} Ni(II) ion was prepared in 2.5% ammonia solution and was diluted to 5.0×10^{-4} mol L^{-1} with 0.10 mol L^{-1} NaOH solution before experiment. MWCNT (diameter: 10–20 nm, length: 1–2 μm, purity > 95%) was purchased from Shenzhen Nanotech Port Co. Ltd. (Shenzhen, China) and used without further purification. Graphite powder (spectral pure) was purchased from Beijing Chemical Reagent Factory (Beijing, China). All the chemicals used were of analytical-reagent

grade. Twice-distilled water was used throughout the experiments.

2.2 Apparatus

Electrochemical measurements were carried out on a CHI 650C electrochemical workstation (Chenhua Instrumental Company, Shanghai, China) controlled by a personal computer. A conventional three-electrode system was employed, including a homemade Ni(II)-MR-MWCNT-PE working electrode, a saturated calomel reference electrode (SCE) and a platinum wire counter electrode. All the potentials quoted in the present work were referred to SCE. All experiments were carried out at room temperature.

2.3 Electrode preparation

The MWCNT-PE was prepared by mixing MWCNT and paraffin oil in a ratio of 3:2 (w/w) in a mortar [26]. A portion of the resulting paste was packed firmly into the cavity (1.6 mm diameter) of a polytetrafluoro ethylene tube. The conventional carbon paste electrode (CPE) was prepared in a similar way by mixing graphite powder with paraffin oil. The electric contact was established via a copper wire. The surface of electrode was smoothed on a weighing paper and rinsed with water. The efficient area of the MWCNT-PE was about 1.94 times as large as that of the CPE using K$_3$Fe(CN)$_6$ as a probe according to Randles–Sevcik equation.

Ni(II)-MR-MWCNT-PE was prepared by the following procedure. MWCNT-PE was placed in 0.10 mol L^{-1} NaOH solution containing 1.0×10^{-3} mol L^{-1} MR and 5.0×10^{-4} mol L^{-1} Ni(II) ion and scanned consecutively between 0.2 and 0.7 V at a scan rate of 0.1 V s^{-1} for 30 cycles. The MR-MWCNT-PE and Ni(II)-MWCNT-PE were prepared by the same way as Ni(II)-MR-MWCNT-PE in 1.0×10^{-3} mol L^{-1} MR and 5.0×10^{-4} mol L^{-1} Ni(II) ion, respectively. Also, the Ni(II)-MR-CPE was prepared by the same way as Ni(II)-MR-MWCNT-PE but the substrate electrode was a CPE.

3 Results and discussion

### 3.1 The preparation and electrochemical behavior of Ni(II)-MR-MWCNT-PE

Consecutive cyclic voltammograms of MWCNT-PE in 0.10 mol L^{-1} NaOH solution containing 1.0×10^{-3} mol L^{-1} MR and 5.0×10^{-4} mol L^{-1} Ni(II) ion are shown in Fig. 1. As shown, an anodic peak at 0.435 V and a cathodic peak at 0.340 V were observed. Peak currents increased gradually with continuous scanning and a
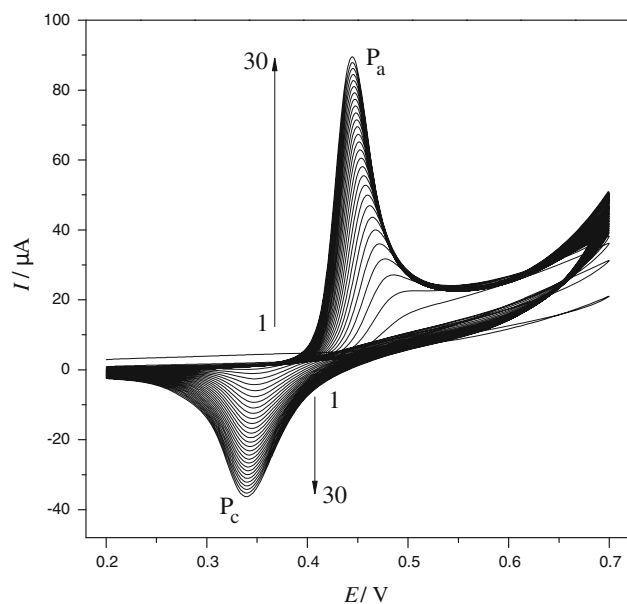
Fig. 1 Multicycle voltamograms of MWCNT-PE in 0.10 mol L^{-1} NaOH solution containing 1.0×10^{-3} mol L^{-1} MR and 5.0×10^{-4} mol L^{-1} Ni(II) ion. Scan rate: 0.1 V s^{-1}, potential range: 0.2–0.7 V

Fig. 2 Cyclic voltammograms of MR-MWCNT-PE (*a*), Ni(II)-MR-MWCNT-PE (*b*) and Ni(II)-MR-CPE (*c*) in 0.10 mol L^{-1} NaOH solution at scan rate of 0.1 V s^{-1}

uniform adherent blue film was observed on the electrode surface. These facts indicated that poly-[Ni(II)-MR] film was deposited on the surface of MWCNT-PE and a Ni(II)-MR-MWCNT-PE was prepared.

Moreover, the voltammetric behavior of Ni(II)-MR-MWCNT-PE was examined and compared with those of MR-MWCNT-PE and Ni(II)-MR-CPE. Figure 2 shows cyclic voltammograms of MR-MWCNT-PE (a), Ni(II)-MR-MWCNT-PE (b) and Ni(II)-MR-CPE (c) in 0.10 mol L^{-1} NaOH solution at a scan rate of 0.1 V s^{-1}. At MR-MWCNT-PE, no electrochemical response was observed. This was due to the passivation of the electrode surface by the irreversibly adsorbed oxidation product of MR. At Ni(II)-MR-MWCNT-PE, a pair of well defined redox peaks with large peak current response ($I_{pa} = 87.6$ μA) and small peak potential separation ($\Delta E_p = 95$ mV) were observed. However, at Ni(II)-MR-CPE, the current response was smaller ($I_{pa} = 32.1$ μA) and the peak potential separation was larger ($\Delta E_p = 99$ mV). These results indicated that the anodic and cathodic peaks observed were from the redox reaction of the Ni(III)/Ni(II) couple in the electrode surface. Also, the reversibility and electrochemical response of Ni(III)/Ni(II) couple in Ni(II)-MR-MWCNT-PE were improved. These characters of Ni(II)-MR-MWCNT-PE resulted from the following contributions. Both MR and its oxidation product acted as ligands for immobilizing Ni(II) ions on the electrode surface. And the presence of MWCNT supplied larger surface area to allow more deposition of poly-[Ni(II)-MR] and to accelerate electron
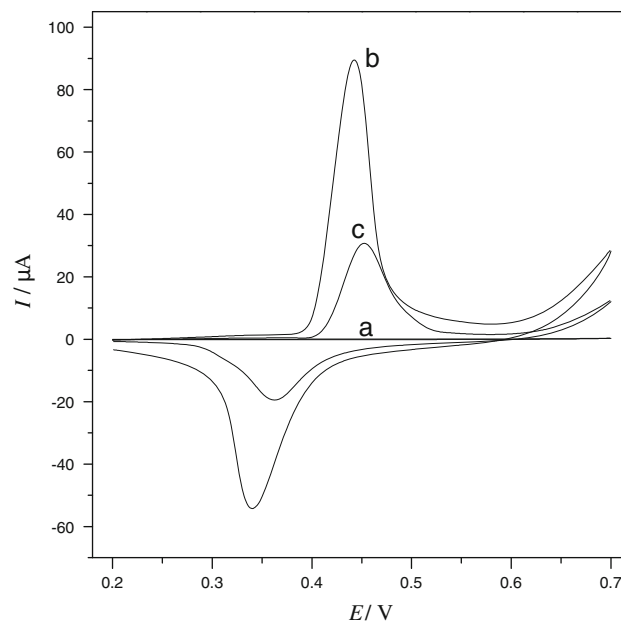
transfer between poly-[Ni(II)-MR] and the substrate electrode. The redox process of the modified electrode was expressed as follows [24, 25]:

$$
\begin{aligned}
&\text{poly - Ni(II)(OH)}_2\text{MR} \\
&\quad + \text{OH}^- \rightleftharpoons \text{poly - Ni(III)(OOH)MR} + \text{H}_2\text{O} + e^- \quad (1)
\end{aligned}
$$

The influence of scan rate v in a wide range of 0.01–1.6 V s^{-1} to the electrochemical behavior of Ni(II)-MR-MWCNT-PE was also investigated (Fig. 3A). As shown, the peak current I_p increased with the increase of scan rate and were proportional to the scan rate v below 0.1 V s^{-1} (Fig. 3B), which indicated a surface confined redox process. According to the following equation [30]:

$$
I_p = \frac{n^2 F^2 v A \Gamma_c}{4RT} \quad (2)
$$

where I_p is the peak current, A is the electrode surface area, the other symbols have their usual meanings, the surface coverage concentration (Γ_c) of the redox couple was calculated to be 2.93×10^{-8} mol cm^{-2}, corresponding to the presence of multilayer of surface species. When $v > 0.1$ V s^{-1}, the peak currents became proportional to the square root of scan rate v (Fig. 3C), signifying the dominance of a diffusion process. This diffuse process was expressed in Eq. 1 and reflected the relatively slower diffusion process of OH$^-$ rather than the charge-transfer process of Ni(III)/Ni(II) couple.

Moreover, at higher scan rates, peak-to-peak separation increased evidently, and the peak potential E_p was proportional to the logarithm of scan rate for $v \geq 0.6$ V s^{-1} (Fig. 3D), indicating the limitation of charge-transfer
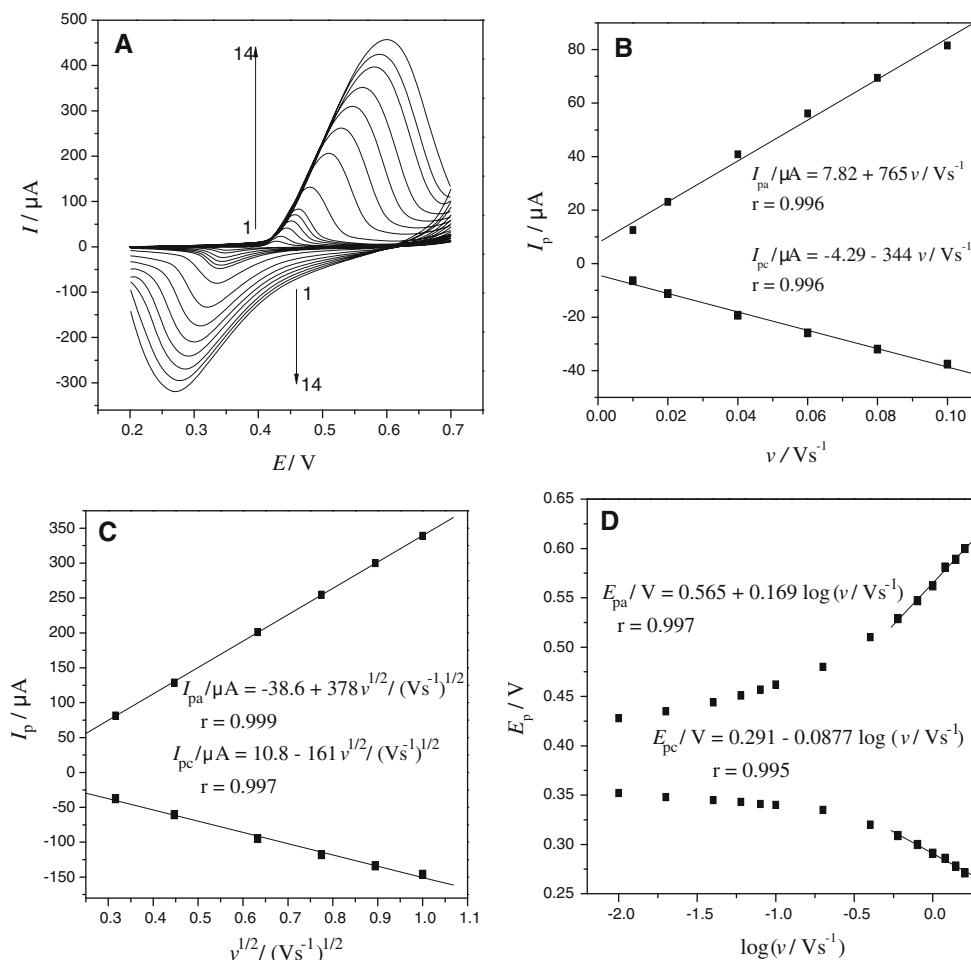
Fig. 3 (**A**) Cyclic voltammograms of Ni(II)-MR-MWCNT-PE in 0.10 mol L^{-1} NaOH solution at various scan rates (from inner to outer): 0.01, 0.02, 0.04, 0.06, 0.08, 0.1, 0.2, 0.4, 0.6, 0.8, 1.0, 1.2, 1.4, 1.6 V s^{-1}. (**B**) Plot of I_p vs. v. (**C**) Plot of I_p vs. $v^{1/2}$. (**D**) Plot of E_p vs. log v

kinetics. Based on the Laviron's theory [31], the electron transfer coefficient α could be calculated. For cathodic and anodic peaks, the slopes of E_p versus log v were −0.088 and 0.169, respectively. The calculated value of α was 0.66. According to the following equation:

$$\log k_s = \alpha \log(1 - \alpha) + (1 - \alpha) \log \alpha - \log(RT/nFv) \\ - \alpha(1 - \alpha)nF\Delta E_p/2.3RT \quad (3)$$

where k_s is the rate constant of electrode reaction and other symbols have their conventional meanings, k_s was calculated to be 1.51 s^{-1}.

3.2 Electrocatalytic oxidation of hydroxylamine at Ni(II)-MR-MWCNT-PE

The voltammetric behaviors of Ni(II)-MR-MWCNT-PE, MWCNT-PE, MR-MWCNT-PE, Ni(II)-MWCNT-PE and Ni(II)-MR-CPE in the absence and the presence of 2.0×10^{-3} mol L^{-1} hydroxylamine are shown in Fig. 4. At
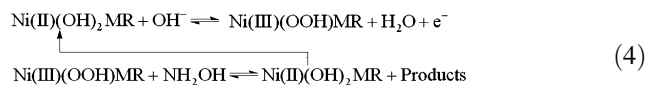
Ni(II)-MR-MWCNT-PE, a pair of redox peaks corresponded to the Ni(III)/Ni(II) couple was observed in the absence of hydroxylamine (Fig. 4A, curve a). After addition of 2.0×10^{-3} mol L^{-1} hydroxylamine, the anodic peak current increased noticeably accompanied by a decrease in cathodic peak current (Fig. 4A, curve b), indicating that Ni(II)-MR-MWCNT-PE had catalytic activity toward the oxidation of hydroxylamine. Under the same experimental conditions, the oxidation of hydroxylamine at MWCNT-PE and MR-MWCNT-PE involved increase in the background current but no defined anodic peaks were observed (Fig. 4B, C). The peak current of the electrocatalytic oxidation of hydroxylamine at Ni(II)-MWCNT-PE and Ni(II)-MR-CPE was 8.61 μA (Fig. 4D, curve h) and 58.5 μA (Fig. 4E, curve j), respectively, which were much lower than that at Ni(II)-MR-MWCNT-PE (159 μA, Fig. 4A, curve b). These results clearly indicated that poly-[Ni(II)-MR] and MWCNT composite material could improve the characteristic of hydroxylamine oxidation. The catalytic center was the Ni(III)/Ni(II)
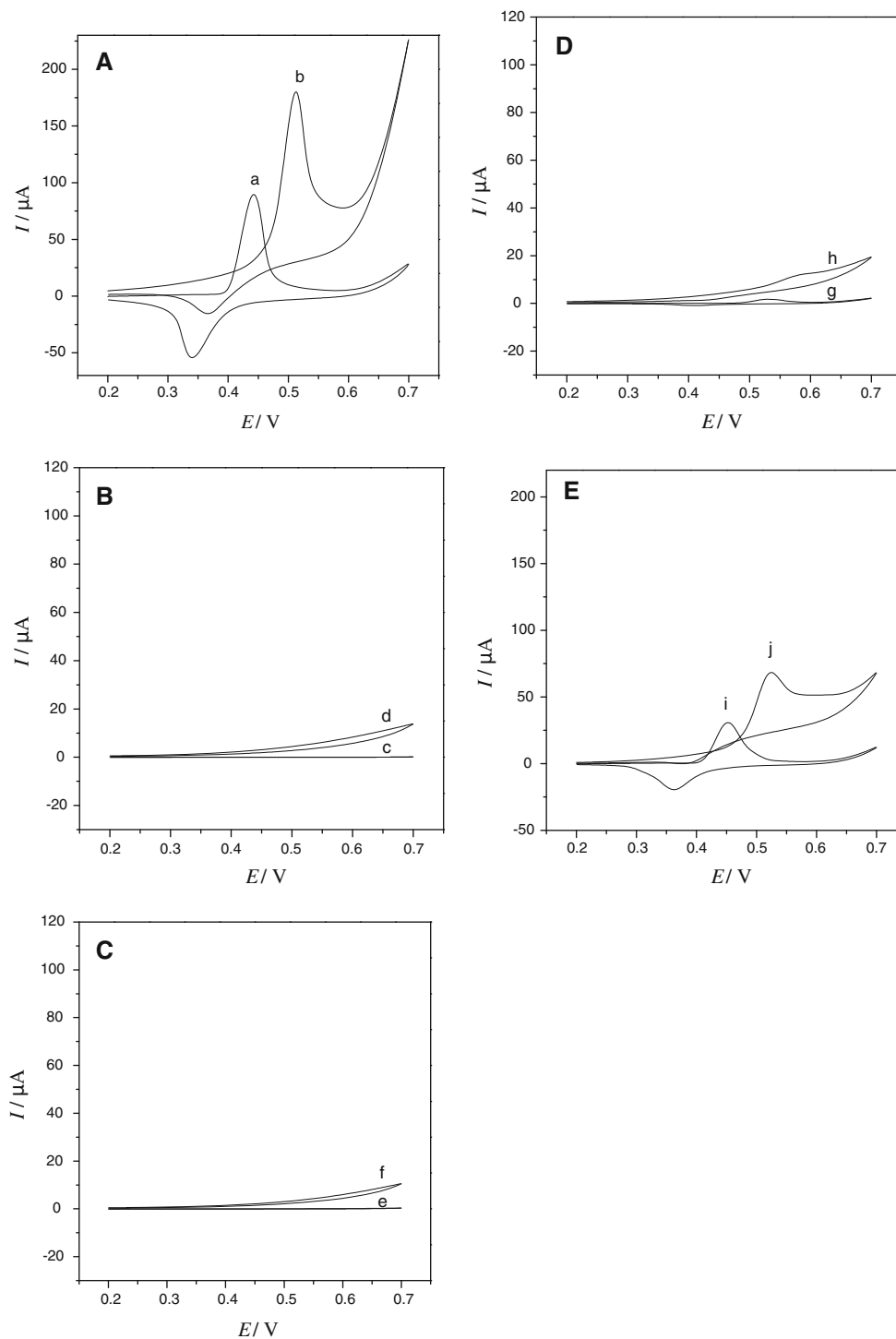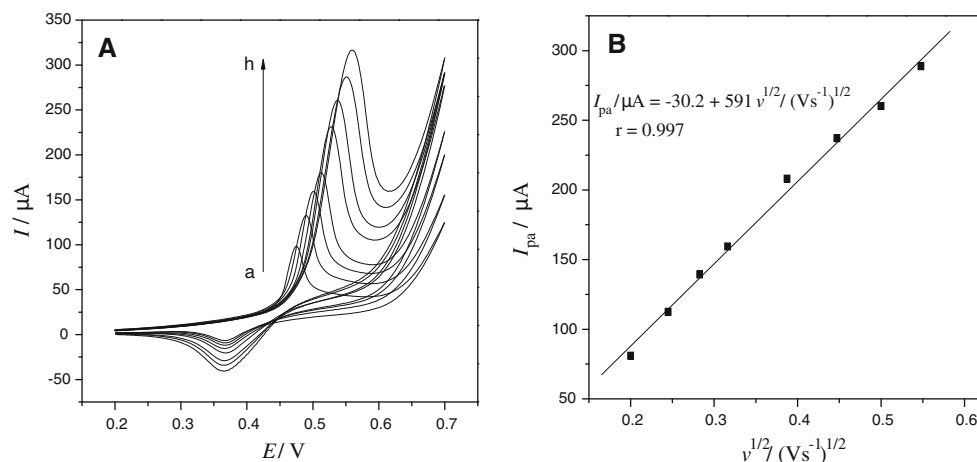
Fig. 4 Cyclic voltammograms of (**A**) Ni(II)-MR-MWCNT-PE, (**B**) MWCNT-PE, (**C**) MR-MWCNT-PE, (**D**) Ni(II)-MWCNT-PE and (**E**) Ni(II)-MR-CPE in the absence (*a, c, e, g, i*) and the presence (*b, d, f, h, j*) of 2.0×10^{-3} mol L^{-1} hydroxylamine in 0.10 mol L^{-1} NaOH solution at scan rate of 0.1 V s^{-1}

couple in the poly-[Ni(II)-MR]. And the oxidation process of hydroxylamine at Ni(II)-MR-MWCNT-PE could be expressed as follows:

$$Ni(II)(OH)_2 MR + OH^- \rightleftharpoons Ni(III)(OOH)MR + H_2O + e^-$$

$$Ni(III)(OOH)MR + NH_2OH \rightleftharpoons Ni(II)(OH)_2 MR + Products \qquad (4)$$

Fig. 5 (**A**) Cyclic voltammograms of Ni(II)-MR-MWCNT-PE in 0.10 mol L^{-1} NaOH solution containing 2.0×10^{-3} mol L^{-1} hydroxylamine at various scan rates (from *a* to *h*): 0.040, 0.060, 0.080, 0.10, 0.15, 0.20, 0.25, 0.30 V s^{-1}. (**B**) Plot of I_{pa} vs. $v^{1/2}$

In addition, the catalytic current of hydroxylamine depended on the pH value. It increased with the increase of pH value from pH 10.00 to 12.50, and reached its maximum value in the range of pH 12.50–13.40. However, no obvious catalytic current was observed when pH < 10.0. Thus, pH 13.0 NaOH solution (0.10 mol L^{-1}) was chosen as supporting electrolyte.

In order to get more information about the catalytic mechanism, cyclic voltammetry and chronoamperometry were conducted.

Cyclic voltammograms of 2.0×10^{-3} mol L^{-1} hydroxylamine at different scan rates v (Fig. 5A) show that the anodic peak currents were proportional to the square root of scan rate v (Fig. 5B). It indicated that at sufficient potential, the electrocatalytic process was controlled by hydroxylamine diffusion to the electrode/solution interface and depended on the hydroxylamine concentration in bulk solution, which was fit for quantitative applications. The

peak potential for the catalytic oxidation of hydroxylamine shifted to more positive values with the increase of scan rate v, suggesting that there was a kinetic limitation in the reaction between the redox sites of poly-[Ni(II)-MR] and hydroxylamine.

Furthermore, chronoamperometry was used for the evaluation of the catalytic rate constant k_{cat} [24]. At intermediate time, when the oxidation current was dominated by the rate of the electrocatalytic reaction of hydroxylamine, the catalytic current I_{cat} could be written as follows:

$$I_{cat}/I_L = \pi^{1/2}(k_{cat}c_0t)^{1/2} \qquad (5)$$

where I_{cat} and I_L are the oxidation currents in the presence and the absence of hydroxylamine, respectively. k_{cat}, c_0 and t are the catalytic rate constant (L mol^{-1} s^{-1}), the bulk concentration (mol L^{-1}) of hydroxylamine and time elapsed (s). From the slope of I_{cat}/I_L versus $t^{1/2}$ relationship
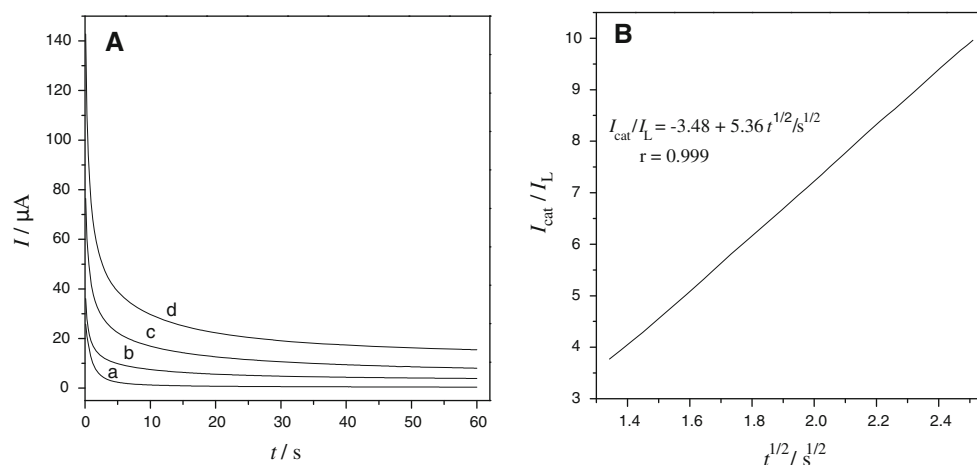
Fig. 6 (**A**) Chronoamperograms of Ni(II)-MR-MWCNT-PE in 0.10 mol L^{-1} NaOH solution containing (*a*) 0, (*b*) 0.5, (*c*) 1.0 and (*d*) 1.5×10^{-3} mol L^{-1} hydroxylamine. (**B**) Plot of I_{cat}/I_L vs. $t^{1/2}$ for 1.0×10^{-3} mol L^{-1} hydroxylamine. Applied potential: +0.55 V

(Fig. 6B), k_{cat} was calculated to be 9.14×10^3 L mol^{-1} s^{-1} for the concentration of 1.0×10^{-3} mol L^{-1} hydroxylamine, which was higher than the reported [23].

## 3.3 Amperometric detection of hydroxylamine at Ni(II)-MR-MWCNT-PE

Based on the voltammetric results described above, amperometric current–time response was recorded to estimate the calibration curve and the detection limit for hydroxylamine determination at Ni(II)-MR-MWCNT-PE. The typical hydroxylamine amperogram during the successive addition of 2.5 μL of 5.0×10^{-3} mol L^{-1} hydroxylamine into continuously stirred 5.0 mL 0.10 mol L^{-1} NaOH solution is shown in Fig. 7. As shown, a well-defined amperometric response with the response time less than 5 s was observed, demonstrating stable and efficient catalytic ability of Ni(II)-MR-MWCNT-PE. The response current was linear with the hydroxylamine concentration from 2.5×10^{-6} to 4.0×10^{-4} mol L^{-1} with a slope of

56.2 mA L mol^{-1} and linear correlation coefficient of 0.999. The detection limit was 8.0×10^{-7} mol L^{-1} ($3\sigma/s$, where σ was the standard deviation of the intercept and s was the slope of the calibration curve). The analytical characteristics of Ni(II)-MR-MWCNT-PE were compared with those reported in the literature, as shown in Table 1.

3.4 Repeatability, reproducibility and stability

The repeatability, reproducibility and stability of the Ni(II)-MR-MWCNT-PE were studied in 0.10 mol L^{-1} NaOH solution. A set of 21 replicate measurements for 2.5×10^{-6} mol L^{-1} hydroxylamine yielded a relative standard deviation (RSD) of 1.9%. Five pieces of Ni(II)-MR-MWCNT-PE were prepared and the RSD for the individual determination of 2.0×10^{-4} mol L^{-1} hydroxylamine was 3.4%. The long-term stability of the modified electrode was tested after stored under dry condition at room temperature for 30 days and no significant change in

Fig. 7 (**A**) Amperometric response of Ni(II)-MR-MWCNT-PE in 0.10 mol L^{-1} NaOH solution by successive addition of 2.5×10^{-6} mol L^{-1} hydroxylamine. Applied potential: +0.55 V. (**B**) Plot of I vs. $c_{hydroxylamine}$
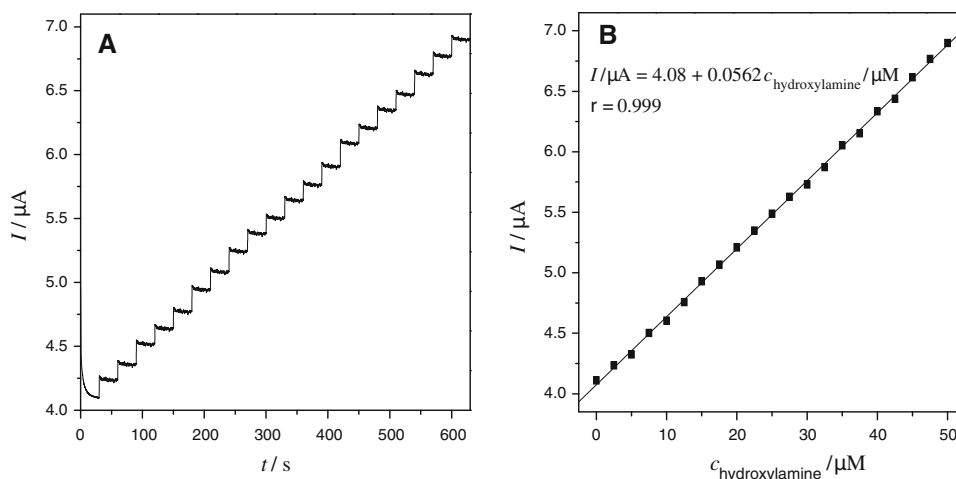
Table 1 Comparison of analytical characteristics of some modified electrodes for the electrocatalytic oxidation of hydroxylamine

Electrode	Linear range (μmol L^{-1})	Detection limit (μmol L^{-1})	Sensitivity (mA L mol^{-1})	Reference
NiCoHCF/GCE[a]	20–200	0.23	4.94	[20]
	200–10000			
CMCPE[b]	60–1000	10.75	0.30	[21]
RMWCNT/GCE[c]	1.0–33.8	1	28.8	[22]
	33.8–81.7			
ARS/GCE[d]	10–800	7.2	73.9	[23]
Ni(II)-MR-MWCNT-PE	2.5–400	0.80	56.2	This work

[a] Hybrid nickel–cobalt hexacyanoferrate film modified glassy carbon electrode

[b] Coumestan derivative modified carbon paste electrode

[c] Rutin multi–wall carbon nanotubes modified glassy carbon electrode

[d] Alizarine red S as a homogeneous mediator

Other symbols had their conversional meanings

Table 2 Results of determination of hydroxylamine in water samples

Sample	Hydroxylamine added (μmol L^{-1})	Hydroxylamine found (μmol L^{-1})[*]	Recovery (%)
Drinking water	5.00	5.10 ± 0.02	102
	10.00	9.94 ± 0.02	199.4
	20.00	19.56 ± 0.01	97.8
River water	5.00	4.81 ± 0.03	96.2
	10.00	10.32 ± 0.02	103
	20.00	19.66 ± 0.03	98.3

[*] Average of five measurements $\pm$ RSD

current responses was observed. Thus, the proposed method exhibited acceptable precision.

3.5 Interferences

In order to evaluate the selectivity of the proposed method, the influence of various substances on the determination of hydroxylamine was studied under the optimum conditions. The tolerable limit was defined as the concentrations of interfering substances that caused an error less than $\pm 5.0\%$ for the determination of 1.0×10^{-5} mol L^{-1} of hydroxylamine. The results showed that 100-fold K^+, NH_4^+, Ca^{2+}, F^-, Cl^-, Ac^-, SO_4^{2-}, PO_4^{3-}, 50-fold Mg^{2+}, Ba^{2+}, Al^{3+}, NO_3^-, SCN^-; 10-fold Pb^{2+}, Fe^{2+}, Co^{2+}, Zn^{2+}, NO_2^-, CO_3^{2-}; 5-fold Cu^{2+}, Fe^{3+} did not interfere with the determination. The results proved that the proposed method had acceptable selectivity.

3.6 Practical applications

The potential application of the proposed method was evaluated by monitoring the concentration of hydroxylamine in water samples. Standard addition method was used for the analysis. The results (shown in Table 2) indicated that the proposed method was suitable for the determination of hydroxylamine in these samples.

4 Conclusions

A new composite material modified electrode Ni(II)-MR-MWCNT-PE was prepared by electrodepositing Ni(II)-MR complex on the surface of MWCNT-PE in alkaline solution. The combination of unique properties of MWCNT and Ni(II)-MR complex resulted in the improvement of both the reversibility and current responses of Ni(II)-MR-MWCNT-PE due to their remarkable synergistic augmentation on the electrochemical responses. The Ni(II)-MR-MWCNT-PE also exhibited electrocatalytic activity toward the oxidation of hydroxylamine. Some kinetic parameters, such as the electron transfer coefficient α, rate constant k_s of the electrode reaction and the catalytic rate constant k_{cat} of the catalytic reaction were calculated. A sensitive amperometric method was proposed for the determination of hydroxylamine with the advantages of fast response, high sensitivity and good reproducibility.

References

1. Kok LDS, Wong YP, Wu TW, Chan HC, Kwok TT, Fung KP (2000) Life Sci 67:91
2. Sies H, Murphy ME (1991) Biology 8:211
3. Alldrick AJ, Flynn J, Rowland IR (1986) Mutat Res 163:225
4. Zhang Q, Wang LF, Li KQ (2002) Chin J Inorg Chem 18:107
5. Zhang Q, Wang LF, Liu YM, Li SB, Wu TX (1997) Chin J Med Chem 7:48
6. Janeiro P, Brett AMO (2005) Electroanalysis 17:733
7. Song YM, Kang JW, Wang ZH, Lu XQ, Gao JZ, Wang LF (2002) J Inorg Biochem 91:470
8. Song YM, Kang JW, Zhou J, Wang ZH, Lu XQ, Wang LJ, Gao JZ (2000) Spectrochim Acta A 56:2491
9. Hofman T, Lees H (1953) Biochem J 54:579
10. Bowman J, Tang L, Silverman CE (2000) J Pharm Biomed Anal 23:663
11. Smith RP, Layne WR (1969) J Pharmacol Exp Ther 165:30
12. Gross P (1985) Crit Rev Toxicol 14:87
13. Dias F, Olojola AS, Jaselskis B (1979) Talanta 26:47
14. Fernando PN, Egwu IN, Hussain MS (2002) J Chromatogr A 956:261
15. Broymann MT, Angells MA, Gordon LI (1982) Anal Chem 54:1209
16. You TY, Wu MJ, Wang EK (1997) Anal Lett 30:1025
17. Canterforf DR (1978) Anal Chim Acta 98:205
18. Zhao C, Song J (2001) Anal Chim Acta 434:261
19. Karabinas G (1985) J Electroanal Chem 189:155
20. Shi LH, Wu T, He P, Li D, Sun CY, Li JH (2005) Electroanalysis 17:2190
21. Zare HR, Nasirizadeh N (2006) Electroanalysis 18:507
22. Zare HR, Sobhani Z, Mazloum-Ardakani M (2007) Sens Actuators B 126:641
23. Mazloum-Ardakani M, Karimi MA, Mirdehghan SM, Zare MM, Mazidi R (2008) Sens Actuators B 132:52
24. Zheng L, Zhang JQ, Song JF (2009) Electrochim Acta 54:4559
25. Majdi S, Jabbari A, Heli H, Moosavi-Movahedi AA (2007) Electrochim Acta 52:4622
26. Rubianes MD, Rivas GA (2003) Electrochem Commun 5:689
27. Sun W, Li Y, Duan Y, Jiao K (2009) Electrochim Acta 54:4105
28. Fang B, Shen RX, Zhang W, Wang G, Zhang C (2009) Microchim Acta 165:231
29. Wan Q, Wang X, Yu F, Wang X, Yang N (2009) J Appl Electrochem 39:785
30. Prodromidis MI, Veltsistas PG, Karayannis MI (2000) Anal Chem 72:3995
31. Laviron E (1979) J Electroanal Chem 101:19